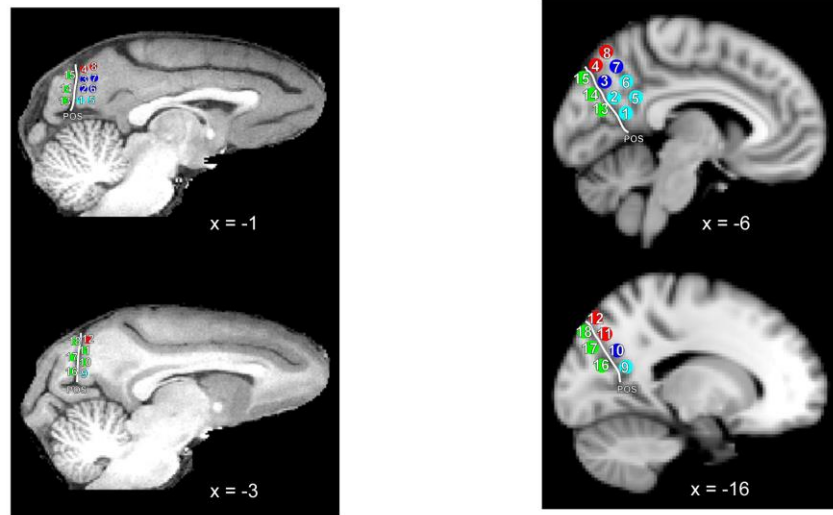


SUPPLEMENTARY MATERIAL

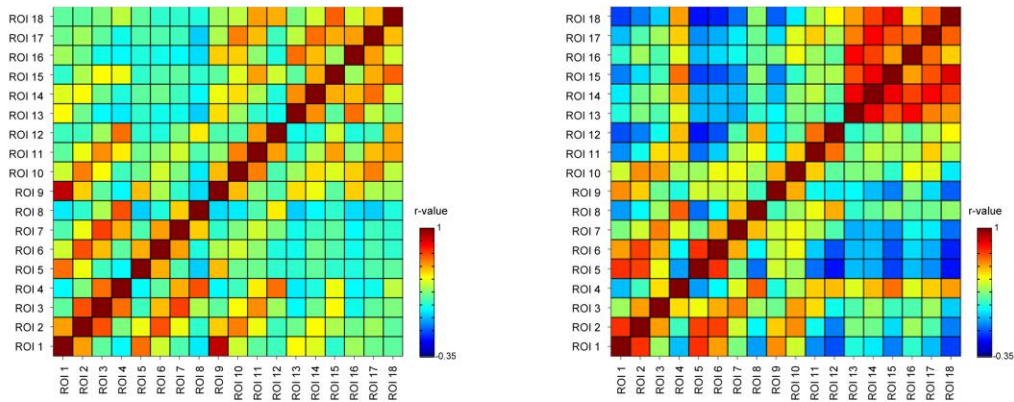
Functional subdivisions of medial parieto-occipital cortex in humans and nonhuman primates using resting state fMRI

R. Matthew Hutchison, Jody C. Culham, J. Randall Flanagan, Stefan Everling and Jason P. Gallivan

A Seed Regions



B Temporal Relationships



C Hierarchical Clustering

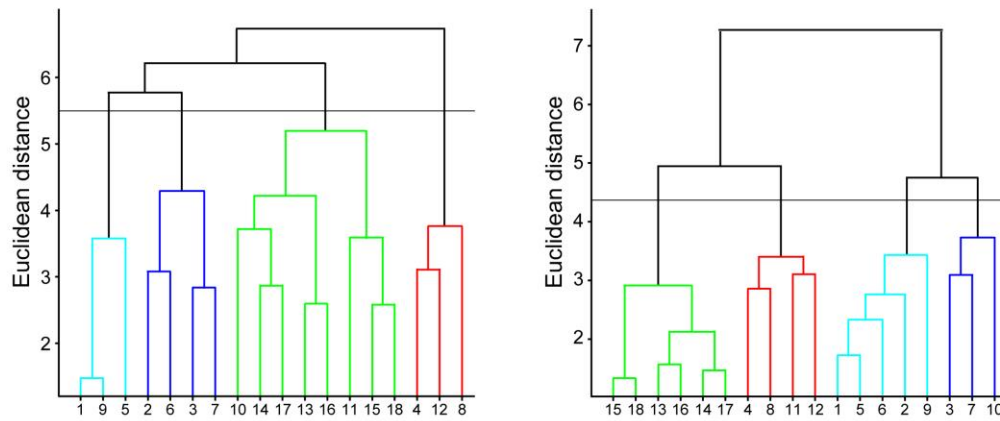


Figure S1: Inclusion of global mean signal regression (GMSR) in data preprocessing produces near identical results. Shown here are the results of including GMSR in the same left hemisphere analysis as performed in Figure 2. **A-C)** Seed ROIs, correlation coefficients and dendrogram plots are shown the same as in Figure 2.

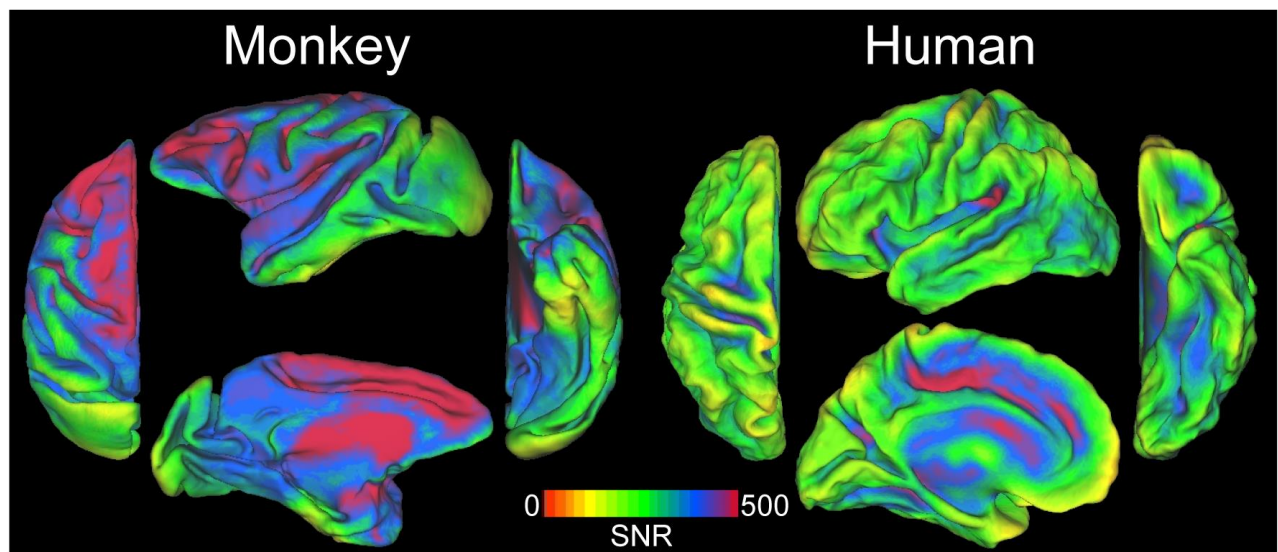
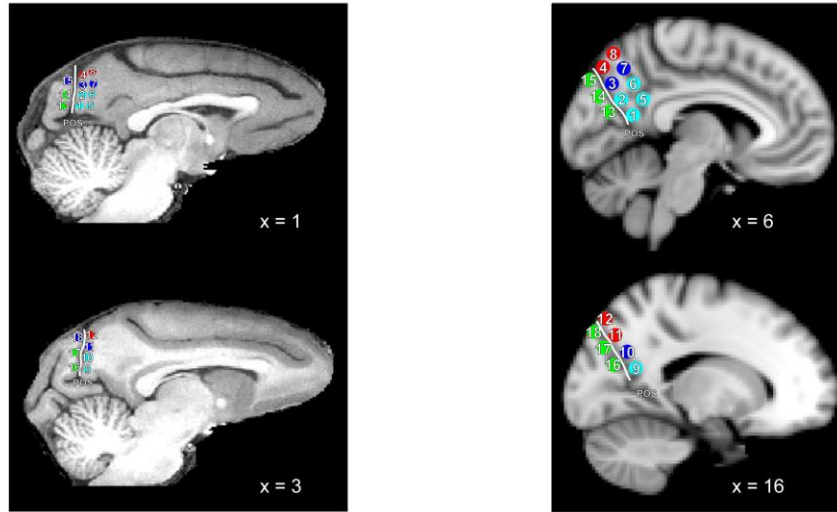
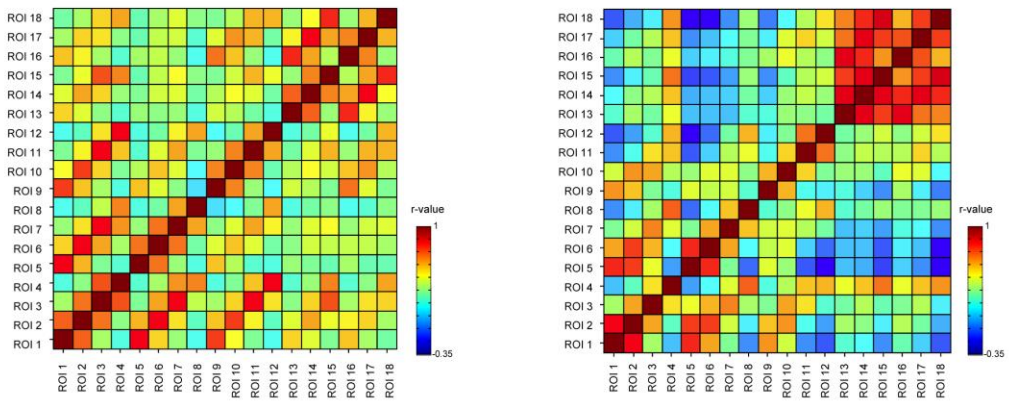


Figure S2: Maps of signal-to-noise ratio (SNR) of the BOLD fMRI data for the macaque (left) and human (right). The mean SNR maps are shown for multiple views of the left hemisphere in the macaque F99 (left; Van Essen 2004) and human PALS-B12 (right; Van Essen 2005) template, respectively. Note that both species generally exhibit SNR values > 100 across the entire brain.

A Seed Regions



B Temporal Relationships



C Hierarchical Clustering

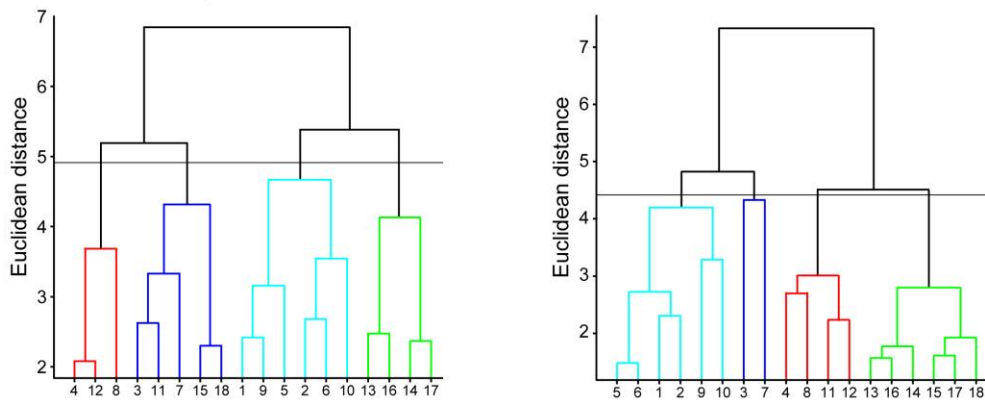
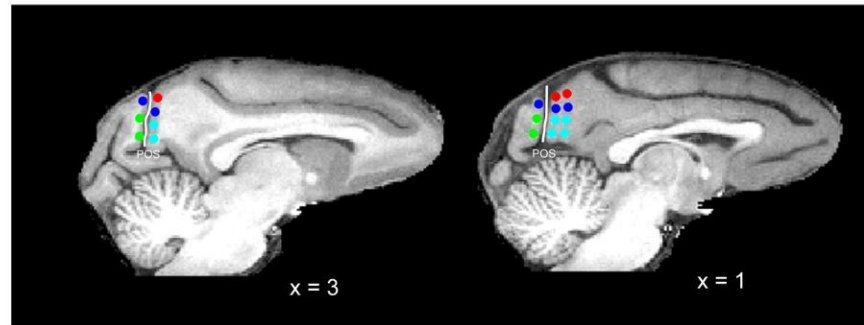


Figure S3: Analysis of macaque and human mPOC seed ROIs for the right hemisphere. A-C) Seed ROIs, correlation coefficients and dendrogram plots are shown the same as in Figure 2.

A Seed Regions



B Associated Whole-Brain Networks

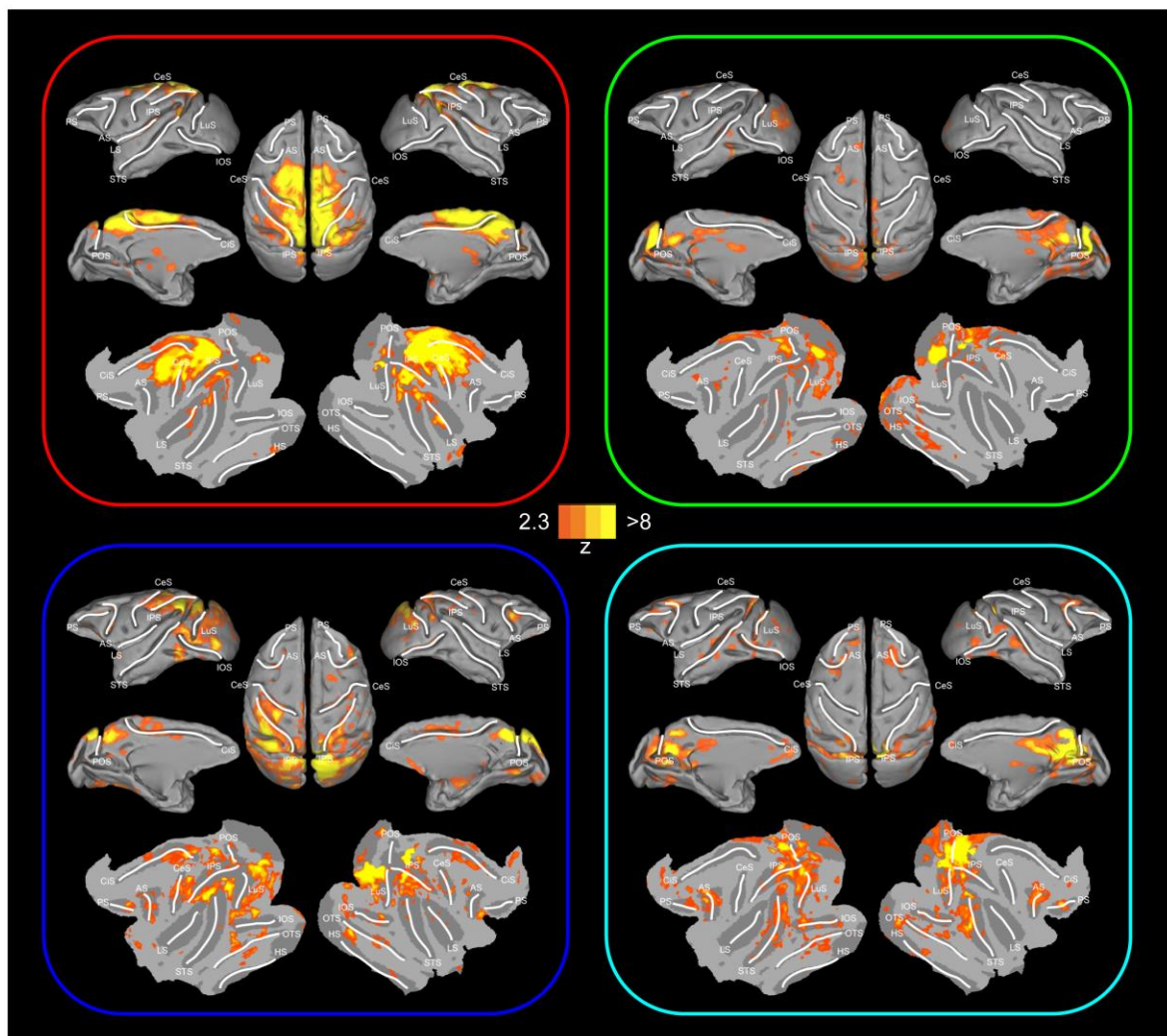
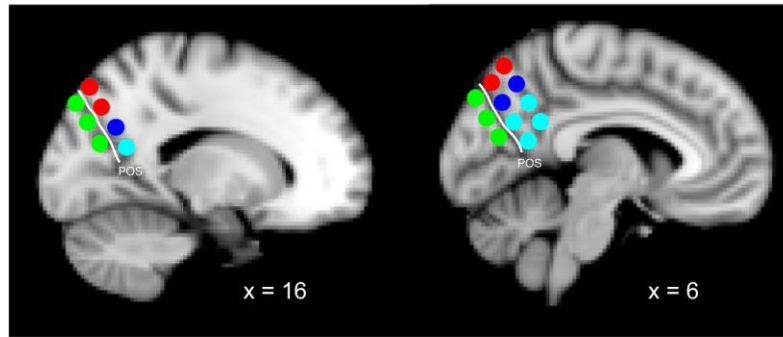


Figure S4: Networks representing the shared connectivity of macaque monkey right hemisphere mPOC seed ROIs within each identified cluster in Figure S1. A-B) ROIs and cluster networks are reported the same as in Figure 3.

A Seed Regions



B Associated Whole-Brain Networks

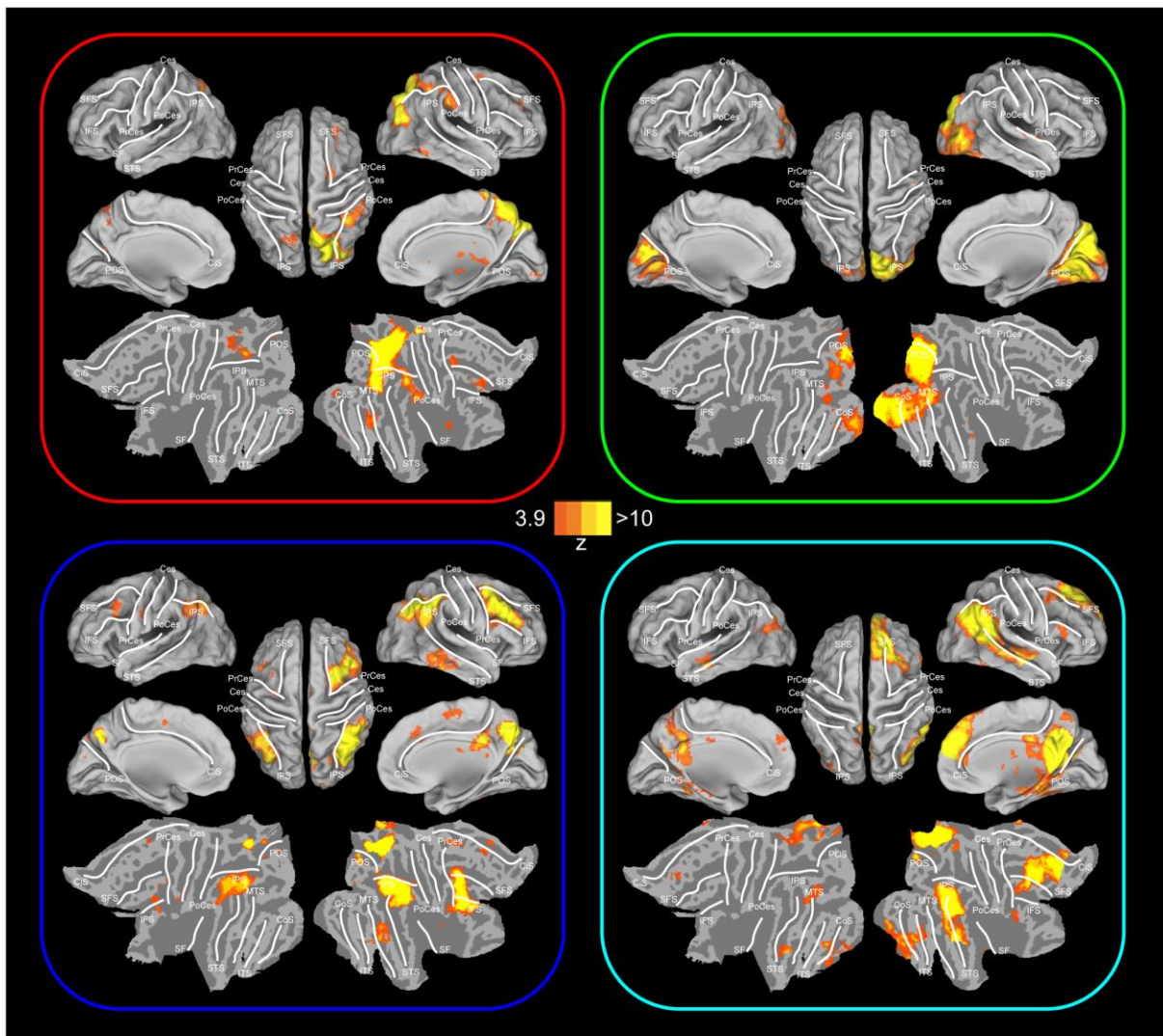


Figure S7: Networks representing the shared connectivity of human right hemisphere mPOC seed ROIs within each identified cluster in Figure S1. A-B) ROIs and cluster networks are reported the same as in Figure 3.

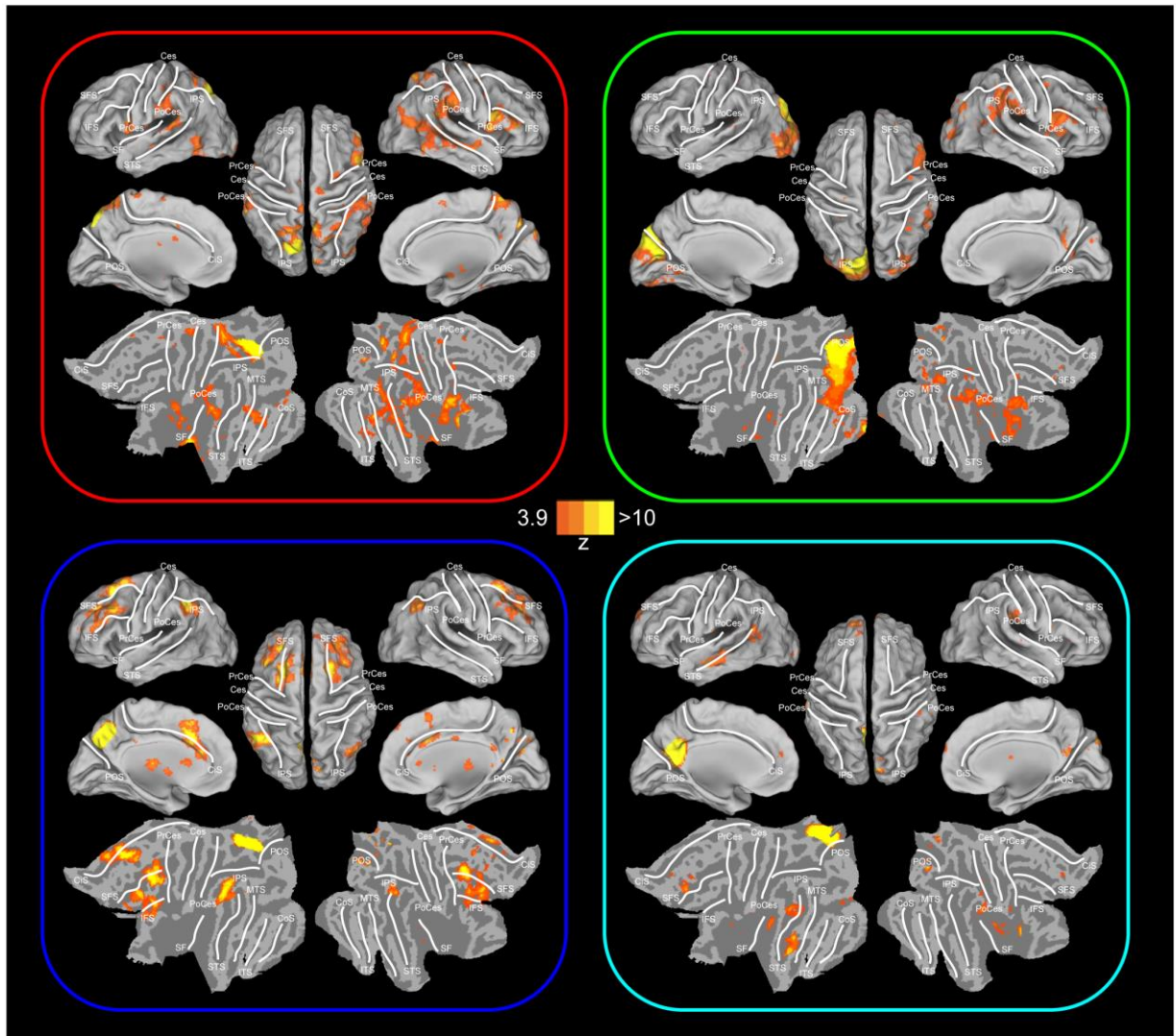


Figure S8: Contrast of the shared network connectivity in the human for the left versus right hemisphere mPOC seed ROIs. Each group of activation maps shows the results of a direct contrast between the whole-brain functional connectivity networks for the left versus right hemisphere seed ROIs identified as being part of each cluster (i.e., the clusters identified in Figure 2C and Figure S3C).

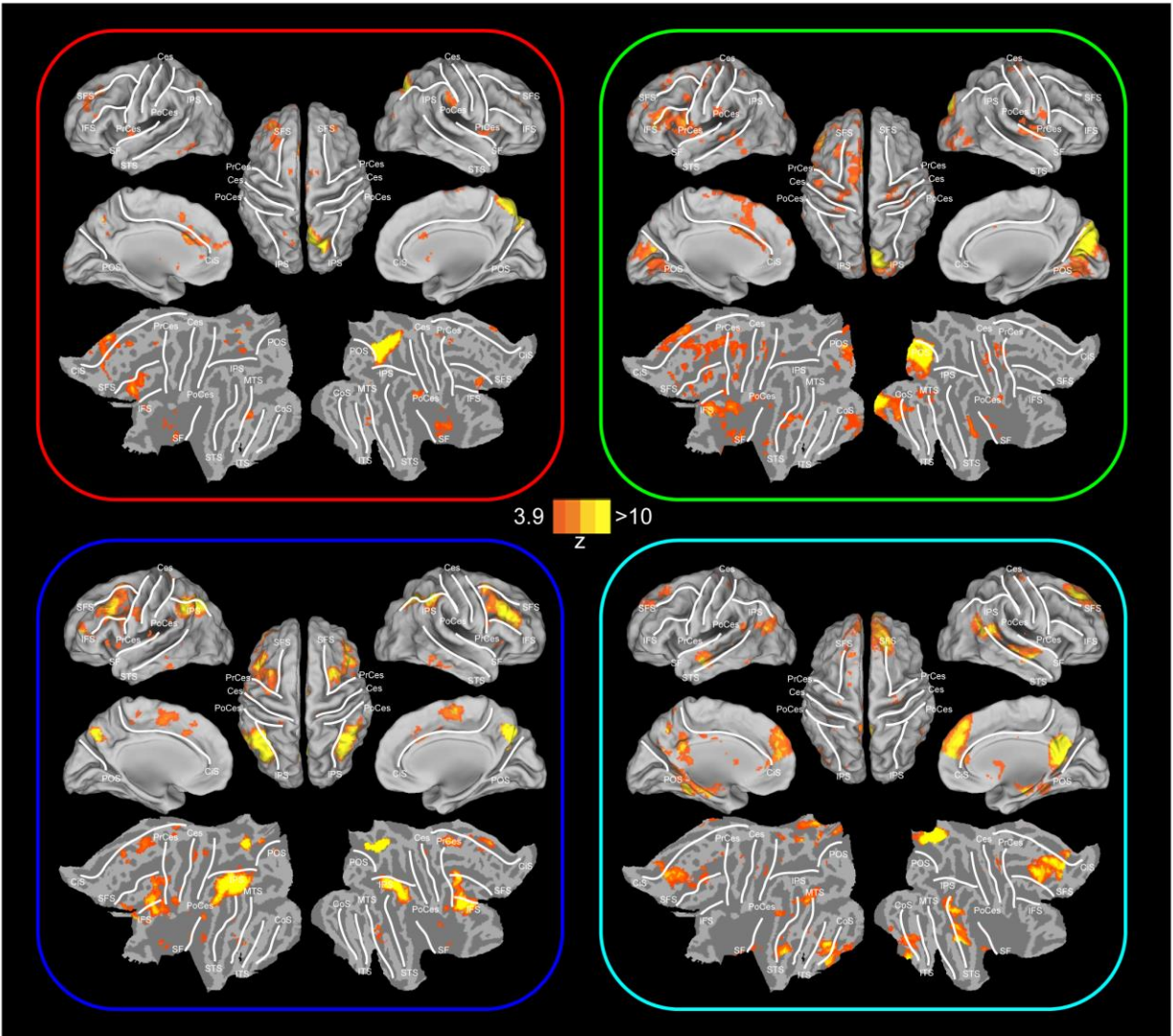


Figure S9: Contrast of the shared network connectivity in the human for the right versus left hemisphere mPOC seed ROIs. Each group of activation maps shows the results of a direct contrast between the whole-brain functional connectivity networks for the right versus left hemisphere seed ROIs identified as being part of each cluster (i.e., the clusters identified in Figure 2C and Figure S3C).

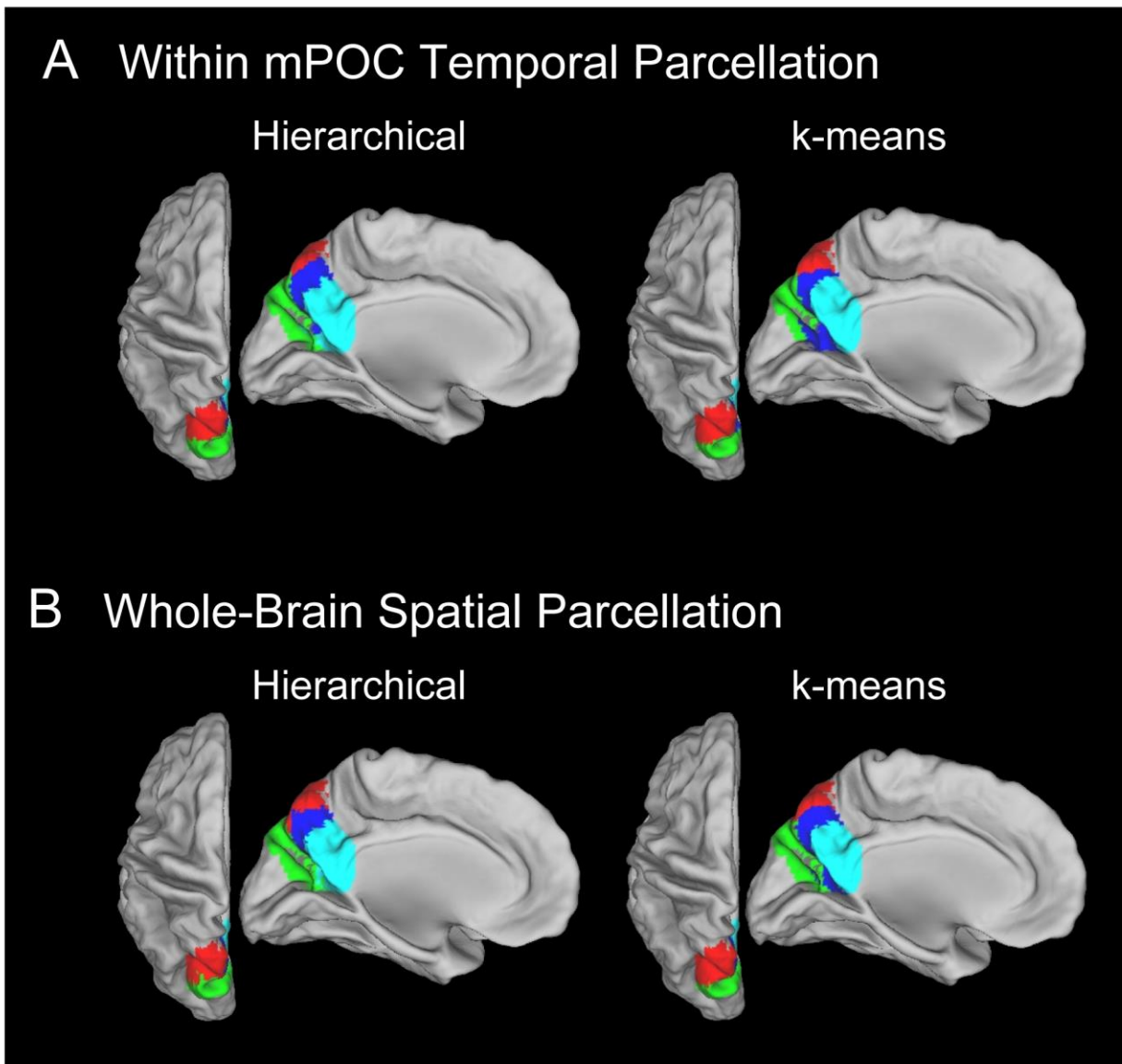


Figure S10: Comparison of Hierarchical versus K-means clustering of mPOC voxels. A) Voxel-wise hierarchical (left) and k-means (right) cluster analysis results for a 4-cluster solution, based on temporal correlations within left hemisphere mPOC, displayed on the dorsal and medial cortical representations of the left hemisphere in the human. **B)** Results of hierarchical (left) and k-means (right) voxel cluster analysis for a 4-cluster solution, based on based on spatial correlations in the whole-brain functional connectivity maps of mPOC voxels, displayed the same as in A. Both cluster analyses show a similar parcellation of mPOC, with the exception that k-means tends to link the middle aPOS (blue cluster) with the ventral extent of the POS.

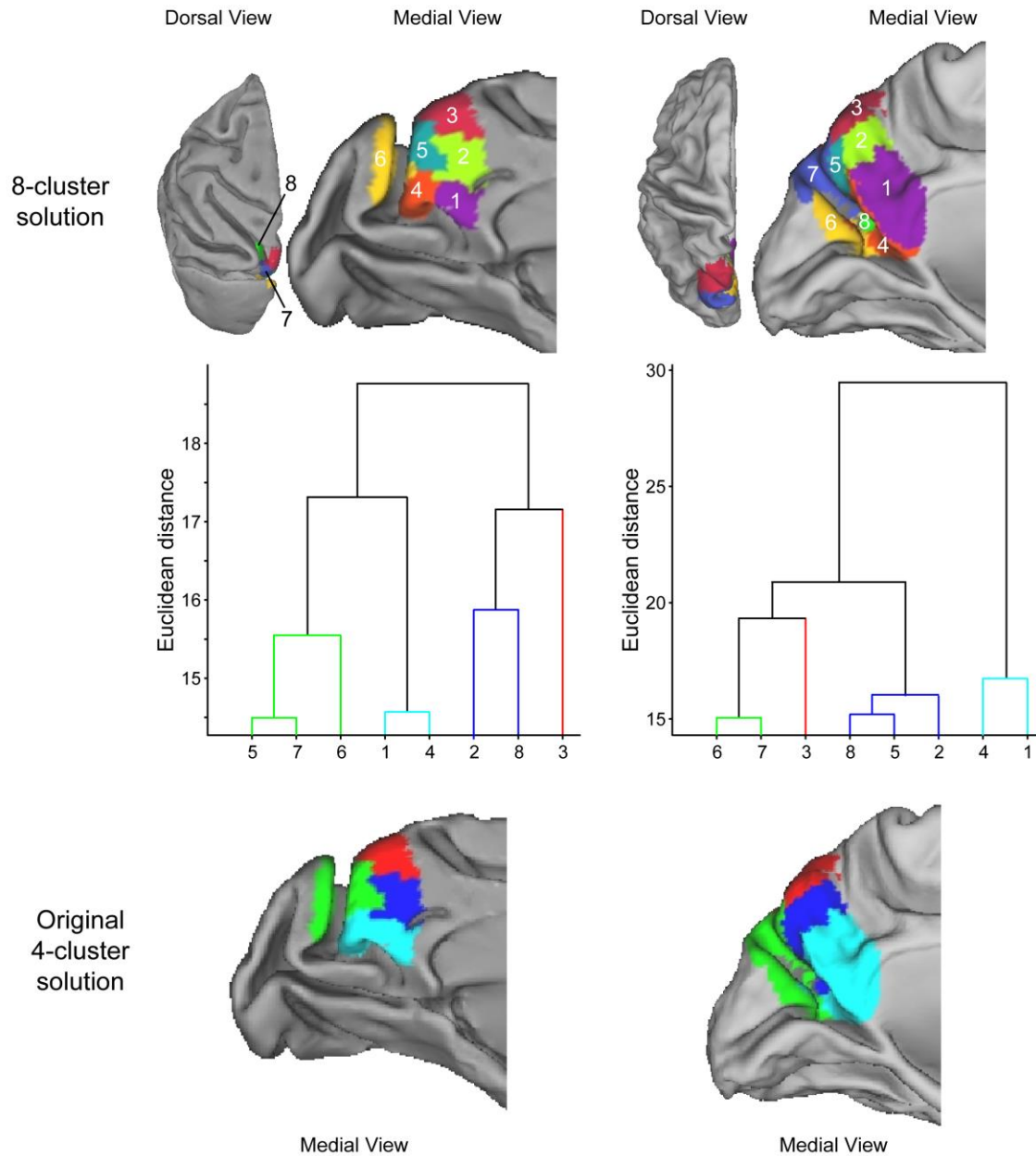


Figure S11: 8-cluster parcellation of mPOC voxels. Top panels show the optimal 8-cluster solution, based on hierarchical voxel-wise clustering of temporal correlations within left hemisphere mPOC, for both the macaque monkey (left) and human (right). Results are displayed on the dorsal and medial cortical representations of each species. Middle panels show dendrogram plots, for both the macaque (left) and human (right), of the hierarchical binary cluster tree of mPOC clusters corresponding to the 8-cluster solution shown at top. Note that lower branches of the dendrogram plot are color-coded to correspond with the parcellations found with the original 4-cluster solution reported in the main manuscript. For visual comparison, the bottom panel shows this original 4-cluster solution.

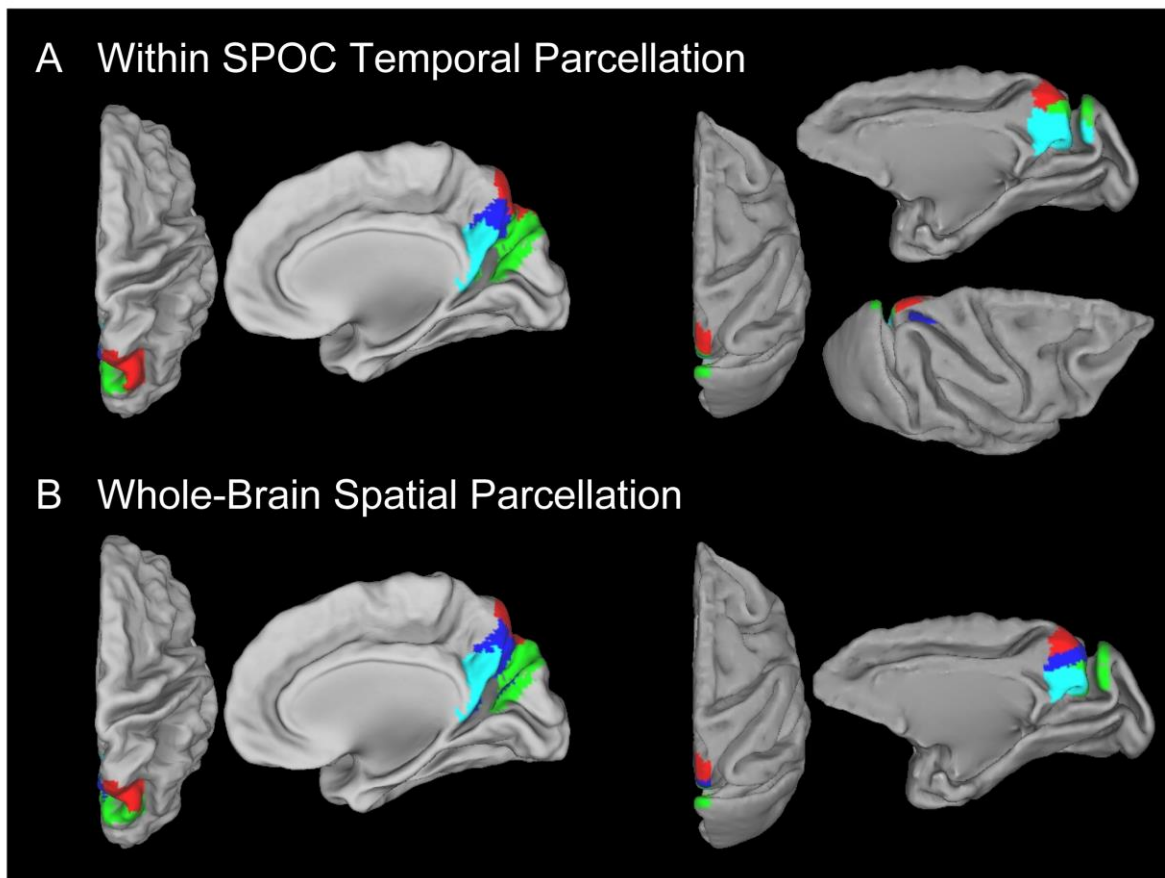


Figure S12: Resting state-based cluster analyses of right hemisphere mPOC voxels in both the human and macaque monkey. A) Results of voxel cluster analysis for a 4-cluster solution, based on temporal correlations within mPOC, displayed on the dorsal and medial cortical representations of the right hemisphere in both the human (left) and macaque monkey (right). Note that the cluster solution of the macaque qualitatively differed from that of the left hemisphere (Figure 4) and that of the whole-brain spatial correlations (shown in B). To highlight this difference, another dorsal view, showing the medial IPS, is shown. **B)** Results of voxel cluster analysis for a 4-cluster solution, based on spatial correlations in the whole-brain functional connectivity maps of mPOC voxels, displayed the same as in A.